Comparison Of Anti-Windup Alternatives For Parallel Controllers

Cristina González Moral
R&D department
Elinsa - Amper
Oviedo, Spain
cgonzalez@elinsa.org

Diego Fernández Laborda
Dept. of Electrical Engineering
University of Oviedo
Gijón, Spain
dflaborda@uniovi.es

Juan M. Guerrero Muñoz
Dept. of Electrical Engineering.
University of Oviedo
Gijón, Spain
guerrero@uniovi.es

Carlos Rivas
R&D department
Elinsa - Amper
La Coruña, Spain
crivas@elinsa.org

David Diaz Reigosa
Dept. of Electrical Engineering
University of Oviedo
Gijón, Spain
diazdavid@uniovi.es

***Abstract*—Parallel controller structures are broadly used for controlling electrical variables in distorted grids and other applications such as electric drives. Each controller in the structure ideally regulates a single harmonic component. In the event of controller output saturation, some anti-windup strategy must be implemented to ensure a correct operation of the controller and a fast and smooth transition from saturated to non-saturated state. The anti-windup techniques proposed for single controller structures can be applied to parallel structures. However, two options exist: 1) Consider the controllers in the parallel structure as independent units during saturation; 2) Consider the parallel controller structure as a whole. The first one is broadly used while the second one has been recently proposed. This paper analyzes the implementation differences and the performance of both solutions in different scenarios: grid-forming and grid-feeding applications.**

***Index Terms*—Realizable references, grid feeding, grid forming.**

I. Introduction

A high percentage of non-linear loads are present in grids and micro-grids. They inject a significant amount of current harmonic content that can eventually distort the grid voltage, increasing the Total Harmonic Distortion (THD) above the admissible values given by regulations and standards [1]–[3]. Harmonic compensation can be implemented using dedicated devices, as passive filters or centralized Active Power Filters (APF) [4], [5]. Since the interface of Distributed Power Generation Systems (DPGSs) is generally based on power converters, this also has opened opportunities for harmonic compensation both in grid forming [6], [7] and grid feeding [3], [8]–[10] converters.

Parallel controller structures are often used for controlling different harmonic components in voltage or current controllers. The discussion will be focused on complex vector current controllers within this paper, although the results can be later extended to both voltage and single-phase controllers. The operation of the parallel controller structures under saturation must be correctly addressed to minimize either the voltage/current THD or the decrease of the fundamental component magnitude. When output saturation is detected in the controller, a two-stage process is needed, as seen in Fig. 1 for a single current controller: a) Saturation: to decide the output voltage vector ($u_s[z]$) within the voltage limits to replace the actual controller output ($u[z]$); b) Anti-windup: to properly saturate the controller to prevent it from working with nonlinear states. For the sake of simplicity, no special notation is given to the complex vector variables.

The hexagon with radius $\frac{2}{3}V_{dc}$ and apothem $\frac{V_{dc}}{\sqrt{3}}$ in Fig. 2 represents the maximum allowable voltage range when using a three-phase inverter, where V_{dc} is the dc-link voltage. Any voltage command (u) that gets outside the voltage hexagon limits (e.g. u_1) must be limited in amplitude and/or distorted in phase. While the hexagon limitation maximizes the inverter voltage utilization, it brings several drawbacks, as implementation complexity, reference frame dependence, and the injection of additional harmonics when the voltage moves along the hexagon sides. An alternative often selected as the limit is using the hexagon inscribed circle seen in Fig. 2. To achieve those limits either Sinusoidal PWM (SPWM) with

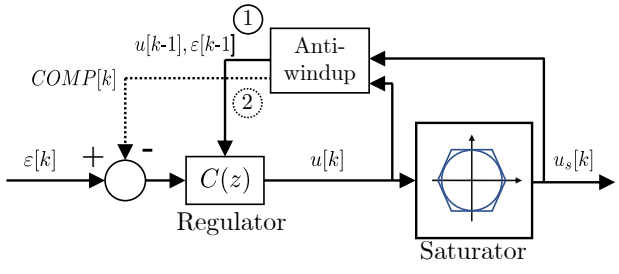

Fig. 1. Saturation and anti-windup conceptual representation for a single controller structure. Two anti-windup alternatives are shown: ① Realizable reference, ② Back-tracking calculation.

This work was supported in part by the Research, Technological Development and Innovation Programs of the Spanish Ministry of Science and Innovation, under grant PID2019-106057RB-I00

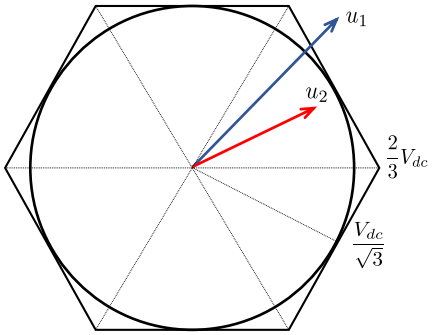

Fig. 2. Complex vector voltage limits, hexagon and circle saturation.

third harmonic injection or Space Vector Modulation (SVM) can be used [11].

The selection of the different saturation methods will depend on the application (grid feeding, APFs, grid forming...), and it is mainly determined by the current/voltage THD or the current/voltage fundamental component magnitude error [3], [5], [7]–[10].

In grid-feeding applications, the goal is to inject an undistorted current into the grid in the presence of grid voltage harmonics. Different alternatives have been proposed, as trajectory analyzers [3], [9], [12], [13] to limit the controller output in case of saturation and avoid harmonic injection, back-tracking schemes that remove low priority harmonics from the compensation [8] or instantaneous methods which estimate trajectories at every time step to avoid overmodulation [10], [14]. APFs need to inject current harmonics into a nonlinear load to remove them from the grid current. In [5], three different instantaneous saturation strategies for APFs are analyzed and compared. Both grid-feeding and APFs applications are mainly oriented to obtain a low THD in the current. In grid-forming applications, both fundamental and harmonic current components need to be injected to obtain a low THD and a low magnitude error in the synthesized voltage. Therefore, the saturation strategies must be different in this case [7].

In addition to the selection of the saturated voltage, some anti-windup technique is needed to allow the controller to operate as in linear region during saturation in order to achieve a fast and bump-less transition from saturated to non-saturated operation [15]. Different strategies have been proposed for single controller systems [15], as the calculation of the realizable reference error, (1) in Fig. 1, error compensation under saturation (back-tracking), (2) (dotted line) in Fig. 1, controller output clamping, integrator clamping, etc.

These anti-windup strategies can be applied to parallel controller structures using any of the two alternatives proposed in the literature that will be described in the next section. This paper will focus on the comparison of both alternatives in different scenarios, as grid forming and grid feeding. This will help to better understand the performance of the existing alternatives which has not been addressed so far. The paper is organized as follows: the alternative methods are described

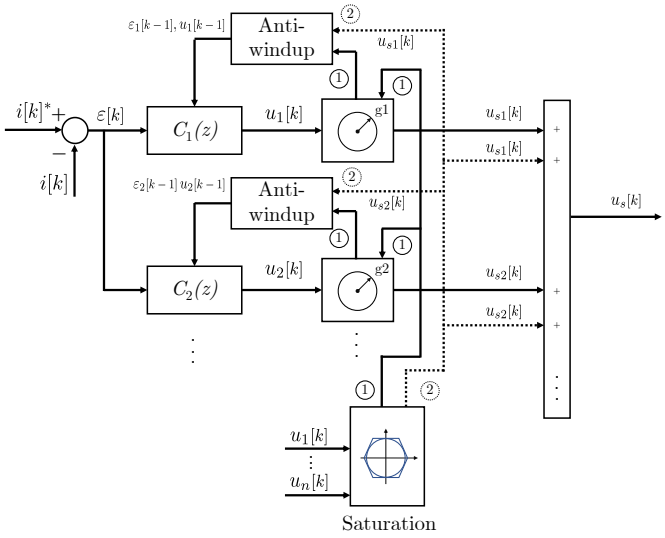

(a)

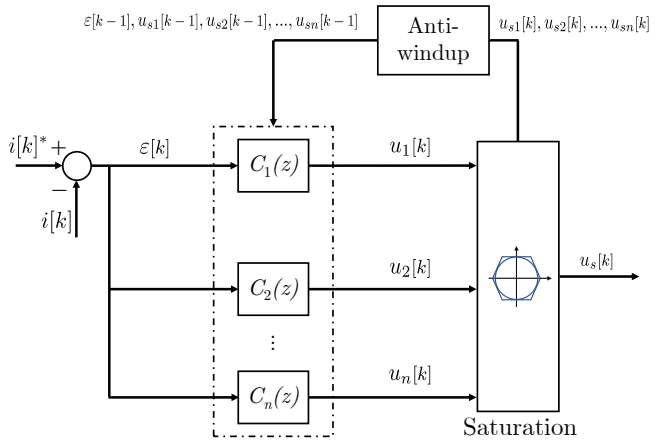

(b)

Fig. 3. Different parallel controllers structures treatment in realizable references anti-windup schemes. a) LAW; b) GAW.

is Section II, simulation results for a grid feeding application and a grid forming application are shown in Section III, and conclusions are presented in Section IV.

II. Anti-windup implementation in parallel controllers

Fig. 3 shows the two alternatives for anti-windup implementation in parallel controller structures. The most often used is shown in Fig. 3(a), that will be herein called "Local anti-windup (LAW)". The output of each individual controller in the structure is compared with their own voltage limit, assigned by some global saturation strategy. If the output surpasses the limit, it is saturated and some anti-windup algorithm as described in Fig. 1 is implemented, as for instance realizable reference as shown in Fig. 3(a). Different saturation alternatives have been proposed belonging to this group. The most simple but inefficient uses pre-defined values for the controller limits (g_1, g_2, ...,g_n) [16]. Others examine the global output vector [5], [8], [17] and recalculate the voltage limits

of each controller [see (1) in Fig. 3(a)] at every control step. Finally, other methods assign the saturated output for each controller at every control step [5], [10], marked as (2) in Fig. 3(a). In any case, the anti-windup is locally applied to each controller. This means that under saturation, each controller in the parallel structure will have a different past-error value. This seems contradictory to the fact that all of them receive the same error at the beginning of each control step, but the impact of this has not been studied so far. It is noted that, in addition to the described anti-windup strategy, some researchers have also proposed to modify the current reference to force the voltage trajectory to avoid saturation in steady-state [3], [9], [10]. However, the analysis made here will be still valid for those methods during the tracking of the optimal trajectory and during load and command transients.

Another alternative shown in Fig. 3(b) has been recently proposed [7], called here "Global anti-windup (GAW)". In this case, the saturated output is also obtained following some strategy and the individual controller saturated outputs are calculated. This is similar to the last type of the aforementioned methods. However, the anti-windup strategy is completely different, since a common past-error is calculated for all the controllers in the parallel structure. This seems more consistent with the fact that the same error is shared among all the controllers. However, any possible improvement of this solution still needs to be proved. The next section shows results of their performance under the same operating conditions in grid feeding and grid forming applications.

III. Method Comparison

As explained in Section I, in grid-forming applications the goal is to generate an undistorted grid voltage in the presence of current harmonics generated by the consumption of the loads. On the contrary, in grid-feeding applications, the goal is to inject an undistorted current into the grid in the presence of voltage harmonics. In the first case, the desired grid voltage will be the output of the converter. In the second case, the minimum voltage generated by the inverter (considering only active power, i.e., injection in phase with the grid) would be the grid voltage. This means that this voltage must be increased in order to generate a voltage difference that (and taking into account the impedance of the filter at the grid's frequency) would generate a current injection into the grid. Both applications are analyzed in the following subsections.

A. Grid forming application

This section contains simulation results for a grid-forming application. Fig. 4 shows a three-phase inverter with an output LC filter, an unbalanced three-phase linear load, and a non-linear load. The main system parameters can be found in Table I. The goal is to obtain a balanced three-phase voltage at the filter output. The THD and fundamental component of this voltage will be used to benchmark the anti-windup schemes.

Since voltage controllers could affect the analysis of the two anti-windup strategies, pre-calculated current commands to ideally achieve a balanced three-phase voltage (400 $V_{\rm rms}$, 50 Hz) at the capacitor will be commanded to the current regulators [7]. This current command is obtained by replacing the inverter and the filter inductor L_f in Fig. 4 by an ideal three-phase voltage source and obtaining the resulting current. In order to track the current command, a parallel current controller structure composed of seven complex vector PI controllers is implemented in stationary reference frame for the fundamental, negative sequence, and the five largest harmonic components (-250, 350, -550, 650, and 950 Hz). A 700 V dc-link voltage ensures a non-saturated operation of the controller obtaining a 1.23% voltage THD and 0% magnitude error in the capacitor voltage.

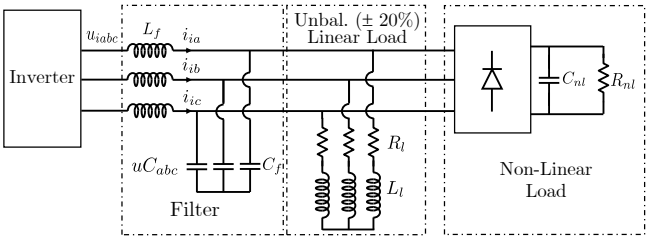

Fig. 4. Test system: Grid forming scenario including unbalanced and non-linear loads.

TABLE I
System Parameters for a Grid Forming Application

Rated voltage	V_r	400 $V_{\rm rms}$	Linear load	L_l	6.6 mH
Rated current	I_r	144 $A_{\rm rms}$	Linear load	Unbalance	±20%
Filter	L	260 µH	Non-linear load	C_{nl}	1 mF
Filter	C	270 µF	Non-linear load	R_{nl}	8.35 Ω
Linear load	R_l	3.36 Ω	Switching Frequency	f_s	10 kHz

Fig. 5 shows the inverter voltage trajectory (in blue) for the current command under the non-linear load conditions. The hexagons in red represents different dc-link voltages: 700 V (non-saturated state), 600, 570 and 540 V (saturated states).

The realizable reference anti-windup technique is implemented for both LAW (Fig. 3a, option (1)) and GAW (Fig. 3b). In both cases, the saturated error ($\varepsilon_{\rm sat}$) is calculated using (1) [7], where $\varepsilon[k]$ is the unsaturated error, $u_{\rm sat}$ is the saturated output of the regulator (coming from the saturation strategy) and $u[k]$ is the unsaturated output of the regulator. In the GAW strategy, b_0 is the sum of the first z-transform numerator coefficient of all the controllers in the parallel

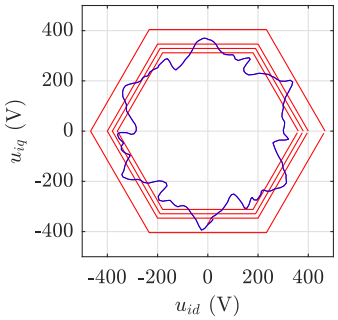

Fig. 5. Grid forming application. Non-saturated inverter voltage trajectory (blue) and hexagon voltage limits (700, 600, 570, 540 V, red).

structure [C_1, C_2... C_n in Fig. 3], while in the LAW strategy the equation is applied individually for each regulator, so b_0 represents just the first z-transform numerator coefficient of the controller.

$$\varepsilon_{\text{sat}} = \varepsilon[k] + \frac{1}{b_0}\left(u_{\text{sat}} - u[k]\right) \tag{1}$$

Both GAW and LAW strategies have been tested with three different saturation alternatives. The first one is termed "Global" (Fig. 6a), in which the output voltage is reduced keeping the original angle (reducing equally all the vector components) [7]. The second saturation technique is called "Magnitude" (Fig. 6c) and is similar to the first method proposed in [5], but also including the fundamental component [7]. In this method, the magnitudes (i.e. not considering the angle) of the voltage vector components from the current controller are added and then compared with the voltage limit. The last technique is called "Group" (Fig. 6b) and corresponds with Method 2 in [5]. In this case, the fundamental component is favored over the rest of the harmonics, to which the "Global" technique is applied. Hexagon or circle voltage limits were considered as indicated in Table II. As explained in Section I, the hexagon limit provides the best voltage utilization at the cost of a higher computational burden. On the other hand, the circle limit provides higher simplicity but worse voltage utilization.

Fig. 7 (LAW) and Fig. 8 (GAW) compare the voltage and current tracking when both methods use the "Global" (hexagon) saturation method during 570 V (0.81 p.u.) dc-link voltage operation and the hexagon voltage limit. Subfigure (a) shows the actual output voltage and the ideal one (dotted line), while (b) shows the actual phase currents and their commands (dotted line), for both Figs. 7 and 8 (GAW). A more accurate current tracking during saturation is seen in the GAW alternative (Fig. 8) with a magnitude error of 7.83% vs.

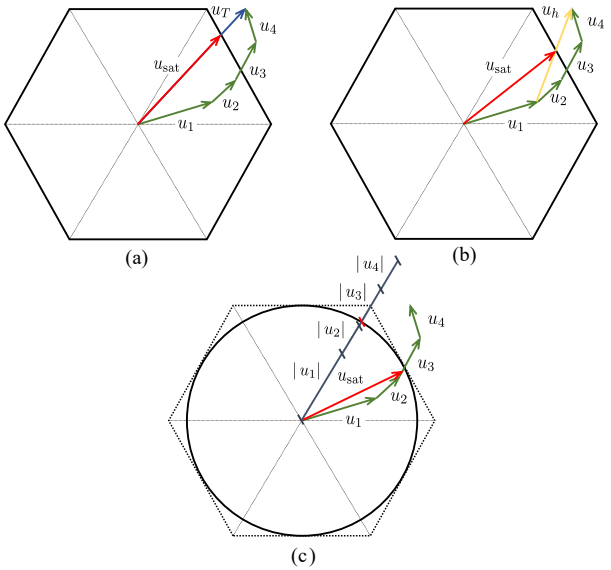

Fig. 6. Saturation methods. (a) "Global". (b) "Group". (c) "Magnitude".

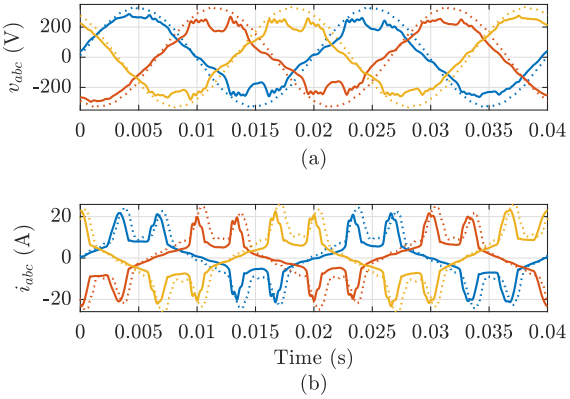

Fig. 7. Grid-formed voltage (a) and phase current tracking (b) during saturation (570 V dc-link) using the "Global (hexagon)" saturation method with LAW. Dotted: current commands. Continuous: Actual currents.

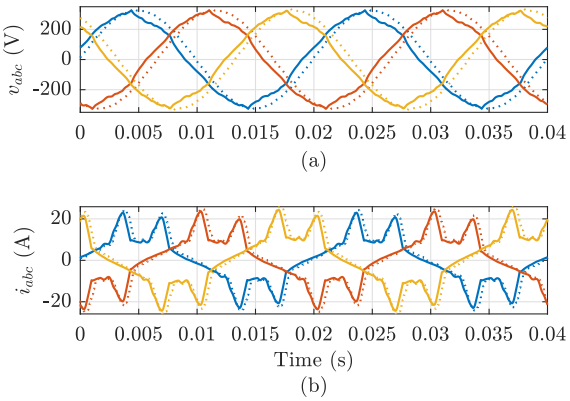

Fig. 8. Grid-formed voltage (a) and phase current tracking (b) during saturation (570 V dc-link) using the "Global (hexagon)" saturation method with GAW. Dotted: current commands. Continuous: Actual currents.

22.35% for the LAW case. The grid-formed voltage distortion is also lower compared with the LAW alternative (Fig. 7), 4.55% in the GAW case vs. 8.99% in the LAW case.

A similar experiment has been repeated for the different cases summarized in Table II for 3 different saturation levels (600, 570 and 540 V), showing both the THD of the voltage at the filter capacitor and the magnitude error of the fundamental component using 3 saturation strategies. In the case of the "Magnitude" technique, only the circle saturation is considered to make it simpler. These results show that the GAW strategy outperforms the LAW one regardless of the saturation strategy in terms of THD (with the only exception being the "Global" (circle) at deep saturation, i.e. 540 V). The "Group" strategy produces a high distortion if combined with LAW, which is especially noticeable at low saturation levels. The magnitude error is also smaller for the GAW strategy except in case the "Group" strategy is adopted. However, the penalty in THD for the LAW strategy is evident in that case. Therefore, it would be advisable to adopt the GAW strategy in most cases regarding grid forming applications.

B. Grid feeding application

This section contains simulation results for a grid-feeding application. Fig. 9 shows a three-phase inverter with an output

TABLE II
GRID FORMING APPLICATION: CAPACITOR VOLTAGE DISTORTION USING DIFFERENT SATURATION STRATEGIES FOR THE DIFFERENT ANTI-WINDUP APPROACHES

Method	600 V		570 V		540 V	
	THD (%)	Mag. Error (%)	THD (%)	Mag. Error (%)	THD (%)	Mag. Error (%)
Global (circle) GAW	2.96	5.20	5.68	9.17	18.59	15.60
Global (circle) LAW	5.48	15.65	8.96	22.34	10.24	27.50
Global (hexagon) GAW	2.80	4.89	4.55	7.83	6.93	10.25
Global (hexagon) LAW	5.46	15.56	8.99	22.35	10.35	28.00
Magnitude (circle) GAW	4.13	15.16	5.59	19.29	7.50	23.13
Magnitude (circle) LAW	10.88	28.86	14.13	34.88	17.63	40.12
Group (circle) GAW	2.63	3.42	3.87	6.85	4.77	10.22
Group (circle) LAW	6.65	1.40	4.85	2.23	5.13	6.49
Group (hexagon) GAW	2.63	3.24	3.82	6.42	4.94	9.56
Group (hexagon) LAW	11.24	0.76	7.80	1.28	6.72	0.12

TABLE III
SYSTEM PARAMETERS FOR A GRID FEEDING APPLICATION

Rated voltage	V_r	400 V_{rms}	Voltage THD	THD_v	$\approx 8\%$
Rated current	I_r	200 A_{rms}	-1^{st} harmonic	h_n	3%
Filter	L	260 µH	-5^{th} harmonic	h_5	5%
Nominaldc-link	V_{dc}	700 V	7^{th} harmonic	h_7	5%
Switching frequency	f_s	10 kHz			

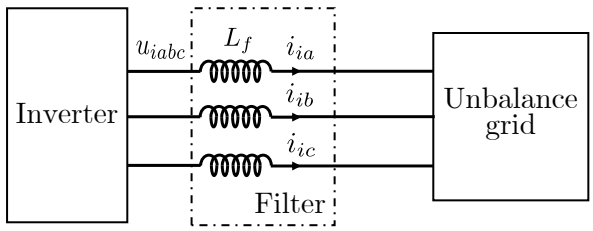

Fig. 9. Test system: Grid feeding scenario with an unbalanced grid.

L filter, connected to an unbalanced grid. The main system parameters can be found in Table III. The goal is to inject a balanced three-phase current to the grid, despite the voltage distortion. The THD and fundamental component of this current will be used to benchmark the anti-windup schemes.

According to the IEEE standard 519-2014 [2], the maximum voltage THD in a grid should not exceed an 8%, while each individual harmonic should remain below a 5%. Due to this, simulations are carried out with around an 8% of grid voltage THD, which would be the worst-case scenario, and 3 different harmonics: -50, -250 and 350 Hz.

In order to track the current command injected to the grid, a parallel current controller structure composed of six complex vector PI controllers is implemented in stationary reference frame for the fundamental, negative sequence, and the most significant first four harmonic components (-250, 350, -550 and 650 Hz). A 700 V dc-link voltage and 200 A peak current reference ensures a non-saturated operation of the controller obtaining a 2% THD and 0% magnitude error in the current through the output inductor.

Fig. 10 shows the inverter voltage trajectory (in blue) for the current command under the distorted grid conditions (in black). The hexagons in red represents different dc-link voltages: 700 V (non-saturated state), 670, 650 and 640 V (saturated states). The particular characteristics of this application results in saturation with a higher voltage in the dc-link compared to the grid forming case.

The realizable reference anti-windup technique is implemented for both LAW (Fig. 3a, option (1)) and GAW (Fig. 3b). In addition, both have been tested with two different saturation alternatives: "Global" (Fig. 6a) and "Group" (Fig. 6c). The "Magnitude" strategy (Fig. 6b) was discarded due to its significantly worse results compared to the other strategies, which causes the algorithm to enter into saturation even at 700 V. This is due to the addition of the magnitude of all the harmonics for the saturation analysis.

Fig. 11 compares the current tracking between the two methods using the "Global" saturation method during 640 V (0.91 p.u.) dc-link voltage operation (hexagon limit). Fig. 11(a) shows the grid voltage with its distortion. Fig. 11(b) and (c) show the current command vs the actual current command for the GAW and the LAW cases, respectively. A more accurate current tracking during saturation is seen in the GAW alternative, also obtaining less inductor current distortion (1.71% vs 2.26% THD).

A similar experiment has been repeated for the different cases summarized in Table IV for 3 different saturation levels (670, 650 and 640 V), showing both the THD of the inverter's current output and the magnitude error of the fundamental current component using two saturation strategies. These results show that the GAW method outperforms the LAW one in the case of the "Global" strategy in terms of THD and current magnitude error. In the case of the "Group" strategy the LAW method behaves better than the GAW method for

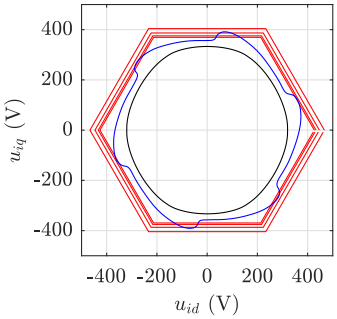

Fig. 10. Grid feeding application. Non-saturated inverter voltage trajectory (blue), hexagon voltage limits (700, 670, 650, 640 V, red) and grid voltage (black).

TABLE IV
GRID FEEDING APPLICATION: INDUCTOR CURRENT DISTORTION USING DIFFERENT SATURATION STRATEGIES FOR THE DIFFERENT ANTI-WINDUP APPROACHES

	670 V		650 V		640 V	
Method	THD (%)	Mag. Error (%)	THD (%)	Mag. Error (%)	THD (%)	Mag. Error (%)
Global (circle) GAW	1.97	0.23	1.74	1.96	1.70	3.00
Global (circle) LAW	2.13	2.37	1.67	2.93	2.38	18.34
Global (hexagon) GAW	1.96	0.1	1.65	1.03	1.71	2.08
Global (hexagon) LAW	1.99	0.28	2.13	2.89	2.26	6.23
Group (circle) GAW	1.75	0.06	5.34	24.93	7.17	41.39
Group (circle) LAW	2.14	2.38	2.21	12.17	2.38	18.31
Group (hexagon) GAW	1.96	0.04	1.84	0.09	2.10	0.34
Group (hexagon) LAW	1.88	0.00	2.14	0.01	2.46	0.00

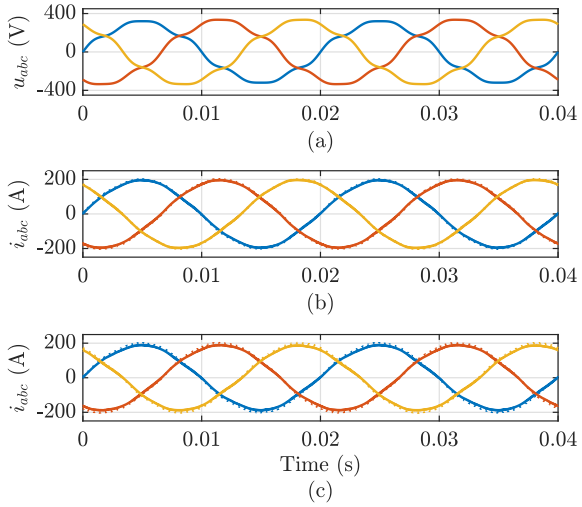

Fig. 11. Grid feeding application. Inverter output voltage and phase current tracking during saturation (640 V dc-link voltage) using the "Global (hexagon)" saturation method. (a) Grid voltage. (b) GAW case. (c) LAW case. Dotted: current commands. Continuous: Actual currents.

higher saturation levels but worse for lower saturation levels. In general, both of them behave far worse than the "Global" strategy. Due to this, the GAW method together with the "Global" strategy would be advisable in the case of grid feeding converters.

IV. CONCLUSION

This paper explores the different performance between local and global anti-windup in parallel controllers under the same operating conditions. Results show a better performance of the GAW approach in terms of output voltage distortion in grid forming converters for all the saturation techniques analyzed.

Regarding grid feeding converters, results are not so straightforward, and the analysis depends on the saturation levels and saturation method employed. In general, results are better with the GAW approach using the "Global" saturation technique. Regarding the "Group" method, results are better with the LAW method, but the performance of the method is worse in general compared to the "Global" case, since this method was proposed for grid forming applications.

REFERENCES

[1] F. Blaabjerg, R. Teodorescu, M. Liserre, and A. V. Timbus, "Overview of Control and Grid Synchronization for Distributed Power Generation Systems," *IEEE Transactions on Industrial Electronics*, vol. 53, no. 5, pp. 1398–1409, Oct. 2006.

[2] "IEEE Recommended Practice and Requirements for Harmonic Control in Electric Power Systems," *IEEE Std 519-2014 (Revision of IEEE Std 519-1992)*, pp. 1–29, Jun. 2014.

[3] M. Rizo, M. Liserre, E. J. Bueno, F. J. Rodríguez, and A. Rodríguez, "Distortion-Free Saturators for Power Converters Under Unbalanced Conditions," *IEEE Transactions on Power Electronics*, vol. 30, no. 6, pp. 3364–3375, Jun. 2015.

[4] M. El-Habrouk, M. Darwish, and P. Mehta, "Active power filters: a review," *IEE Proceedings - Electric Power Applications*, vol. 147, no. 5, pp. 403–413, Sep. 2000.

[5] A. Amerise, M. Mengoni, G. Rizzoli, L. Zarri, A. Tani, and D. Casadei, "Comparison of three voltage saturation algorithms in shunt active power filters with selective harmonic control," *IEEE Transactions on Industry Applications*, vol. 56, no. 3, pp. 2762–2772, May 2020.

[6] R. H. Lasseter, Z. Chen, and D. Pattabiraman, "Grid-forming inverters: A critical asset for the power grid," *IEEE Journal of Emerging and Selected Topics in Power Electronics*, vol. 8, no. 2, pp. 925–935, 2020.

[7] C. G. Moral, J. M. Guerrero, D. Fernández, D. Reigosa, C. Rivas, and F. Briz, "Realizable reference anti-windup implementation for parallel controller structures," *IEEE Journal of Emerging and Selected Topics in Power Electronics (early access)*, pp. 1–1, 2020.

[8] L. Harnefors, A. G. Yepes, A. Vidal, and J. Doval-Gandoy, "Reduction of saturation-induced distortion and antiwindup in multifrequency current control," *European Conference on Power Electronics and Applications (EPE)*, pp. 1–7, Sep. 2015.

[9] ——, "Multifrequency Current Control With Distortion-Free Saturation," *IEEE Journal of Emerging and Selected Topics in Power Electronics*, vol. 4, no. 1, pp. 37–43, Mar. 2016.

[10] J. Moriano, M. Rizo, E. Bueno, J. R. Sendra, and R. Mateos, "Distortion-Free Instantaneous Multifrequency Saturator for THD Current Reduction," *IEEE Transactions on Industrial Electronics*, vol. 66, no. 7, pp. 5310–5320, Jul. 2019.

[11] D. G. Holmes and T. A. Lipo, *"Pulse Width Modulation For Power Converters," 1^{st} edition*. Wiley-IEEE Press, 2003.

[12] A. G. Yepes, J. Doval-Gandoy, and H. A. Toliyat, "Multifrequency Current Control Including Distortion-Free Saturation and Antiwindup With Enhanced Dynamics," *IEEE Transactions on Power Electronics*, vol. 33, no. 9, pp. 7309–7313, Sep. 2018.

[13] A. G. Yepes and J. Doval-Gandoy, "Effective current limitation for multifrequency current control with distortion-free voltage saturation and antiwindup," *IEEE Transactions on Power Electronics*, vol. 35, no. 12, pp. 13 697–13 713, May 2020.

[14] J. Serrano, J. Moriano, M. Rizo, and F. J. Dongil, "Enhanced current reference calculation to avoid harmonic active power oscillations," *Energies*, vol. 12, no. 21, Oct. 2019.

[15] Youbin Peng, D. Vrancic, and R. Hanus, "Anti-windup, bumpless, and conditioned transfer techniques for PID controllers," *IEEE Control Systems Magazine*, vol. 16, no. 4, pp. 48–57, Aug. 1996.

[16] P. Mattavelli, "Synchronous-frame harmonic control for high-performance AC power supplies," *IEEE Transactions on Industry Applications*, vol. 37, no. 3, pp. 864–872, May/Jun. 2001.

[17] T. C. Y. Wang and X. Yuan, "Design of multiple-reference-frame PI controller for power converters," *in 2004 IEEE 35th Annual Power Electronics Specialists Conference (IEEE Cat. No.04CH37551)*, vol. 5, pp. 3331–3335, Jun. 2004.